Journal of Organometallic Chemistry 694 (2009) 2846–2853

Contents lists available at ScienceDirect

Journal of Organometallic Chemistry

journal homepage: www.elsevier.com/locate/jorganchem

Relation between coordination geometry and stereoelectronic properties in DFT models of the CO-inhibited [FeFe]-hydrogenase cofactor

Claudio Greco [a], Maurizio Bruschi [b,*], Piercarlo Fantucci [a], Luca De Gioia [a,*]

[a] Department of Biotechnology and Biosciences, University of Milano-Bicocca, Piazza della Scienza 2, 20126 Milan, Italy
[b] Department of Environmental Sciences, University of Milano-Bicocca, Piazza della Scienza 1, 20126 Milan, Italy

ARTICLE INFO

Article history:
Received 9 February 2009
Accepted 5 March 2009
Available online 13 March 2009

Keywords:
Bioinorganic chemistry
Biomimetic complexes
Iron
Density functional calculations
Hydrogenases

ABSTRACT

In this work DFT has been used to characterize model complexes structurally related to the CO-inhibited form (**Hox-CO**) of [FeFe]-hydrogenases.

The investigation of a recently synthesized diiron complex ($[Fe_2\{MeSCH_2C(Me)(CH_2S)_2\}(CN)_2(CO)_4]^-$, [M. Razavet, S.J. Borg, S.J. George, S.P. Best, S.A. Fairhurst, C.J. Pickett, Chem. Commun. 2002, 700–701]) that closely reproduces most features of the inhibited enzyme cofactor, led to the conclusion that the computation of DFT energy differences, as well as the comparison between computed and experimental IR and EPR spectra, does not allow to confidently distinguish among isomers differing for the position of CO and CN ligands, an issue which is relevant not only to fully understand the mechanism of CO-mediated inhibition of the enzyme, but more generally to further understand the factors affecting substrates coordination to the enzyme active site.

The latter observation prompted us to probe the effect of the electronic properties of ligands on the structural features of a series of $[Fe_2(SCH_2\mathbf{X}CH_2S)(CN)_2(CO)_3(\mathbf{L})]^{n-}$ complexes related to the **Hox-CO** form of the enzyme but differing for the nature of **L** (CO, $(CH_3)_2S$, CH_3S^-, CH_3O^- and F^-) and **X** (CH_2, NH and O). Results revealed that the electronic properties of ligands, as well as the nature of the chelating group bridging the two iron atoms, can affect the coordination geometry of the distal metal center. In particular, it turned out that the inclusion of hard ligands in the Fe coordination sphere could be a viable strategy to selectively favour isomers featuring two CO groups trans to each other. On the other hand, the substitution of propanedithiolate with a di(thiomethyl)amine residue led to the selective stabilization of structures featuring a CN ligand in trans to the μ-CO group, thanks to the formation of an intramolecular hydrogen bond. The relevance of these DFT results for the design of novel biomimetic models of the CO-inhibited [FeFe]-hydrogenases active site is discussed.

1. Introduction

[FeFe]-hydrogenases catalyze the reversible oxidation of molecular hydrogen: ($H_2 \leftrightarrows 2H^+ + 2e^-$), a very simple reaction that could have fundamental importance for the possible future development of a hydrogen-based economy [1].

X-ray crystallographic studies on [FeFe]-hydrogenases from *Clostridium pasteurianum* (CpI) [2] and *Desulfovibrio desulfuricans* (DdHase) [3] have shown that the active site of these enzymes possesses a {2Fe3S} sub-site bearing classical organometallic ligands such as CO and CN^- ligands. The iron atoms of the sub-site are bridged by two sulfur atoms of a 1,3-propanedithiolate (pdt) or a related chelating ligand. One of the iron atoms shares a cysteinyl sulfur ligand with a classical Fe_4S_4 cluster; the resulting iron–sulfur complex is usually referred to as the H-cluster, and the two iron atoms of the {2Fe3S} sub-site are termed "proximal" (Fe_p) or "distal" (Fe_d), depending on their positions with respect to the Fe_4S_4 cluster (Scheme 1).

Direct metal–hydrogen interaction at the sub-site is required for the enzymatic activity of [FeFe]-hydrogenases, and the {2Fe3S} assembly is thought to change redox state along the catalytic cycle [4]. Spectroscopic investigations have revealed that the partially oxidized active (**Hox**) and CO-inhibited (**Hox-CO**, which has an additional carbonyl ligand on Fe_d) forms of the sub-site are paramagnetic ($S = ½$) [5]; recent experimental [6] and theoretical [7,8] studies converge towards the assignment of a Fe(I)Fe(II) redox state for the binuclear subsite in both **Hox** and **Hox-CO**. The investigation of the reaction **Hox** + **CO** → **Hox-CO** has relevant bearings not only for the study of CO-mediated inhibition of the enzyme but also for a more general comprehension of the factors affecting substrates coordination to the H-cluster. Indeed, several

* Corresponding authors. Tel.: +39 02 6448 2816 (M. Bruschi); tel.: +39 02 6448; fax: +39 02 6448 3478 (L. De Gioia).
E-mail addresses: maurizio.bruschi@unimib.it (M. Bruschi), luca.degioia@unimib.it (L. De Gioia).

0022-328X/$ - see front matter © 2009 Elsevier B.V. All rights reserved.
doi:10.1016/j.jorganchem.2009.03.007

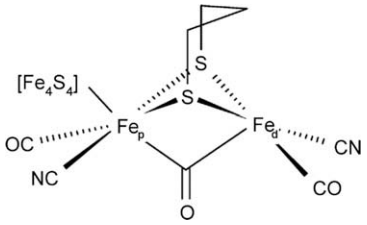

Scheme 1. Structure of the H-cluster in [FeFe]-hydrogenases.

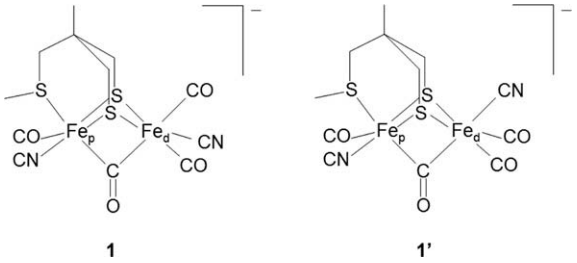

Scheme 3. Schematic structures of isomers **1** and **1′**.

crucial issues related to the **Hox-CO** form are still unclear. As an example, there is still debate about the disposition of ligands around Fe_d in the CO-inhibited enzyme. Zilberman et al. proposed that, in **Hox-CO**, the exogenous CO molecule is bound to Fe_d in *trans* to one of the sulfur atoms of the bidentate ligand included in the {2Fe3S} cluster (Scheme 2, model **A**) [9]. On the other hand, the results of a more recent hybrid quantum mechanical/molecular mechanical (QM/MM) study on an all-atom model of DdHase evidenced that the exogenous CO ligands should bind the Fe_d center in *trans* to the μ-CO group (Scheme 2, model **B**) [10]. In fact, the enzyme form corresponding to **B** was computed to be lower in energy than **A** by 3.34 kcal mol^{-1} when a pdt moiety bridges the metal centers, but the energy gap reduces to 1.43 kcal mol^{-1} when the chelating ligand is di(thiomethyl)amine (dtma) [10]. Since several mechanicistics considerations and spectroscopic results point towards the presence of dtma as the chelating ligand [11], it is not possible to exclude that the *thermodynamic* product of CO-inhibition corresponds to an enzyme form closely resembling **A**, as suggested by Zilberman et al. [9].

As far as the magnetic properties of [FeFe]-hydrogenases in the CO-inhibited form are concerned, it is relevant to note that DdHase and CpI show an axial (or slightly rombic) EPR signal upon CO-mediated inactivation, while CpII – i.e. the second [FeFe]-hydrogenase isoform expressed by *C. pasteurianum* – shows a rhombic EPR signal after reaction with exogenous CO [12]. On the basis of qualitative considerations, it was proposed that such discrepancy in magnetic properties could be due to major differences in the Fe_d coordination sphere, since EPR signals of axial and rhombic form would fit better with H-cluster structures corresponding to model **A** and model **B**, respectively [9]. However, the direct calculation of EPR parameters of these two models suggests that distinguishing between the two isomers of the CO-inhibited enzyme on the basis of their magnetic properties could be a non-trivial task [10].

In such a complicated framework, the design and synthesis of targeted organometallic models of **Hox-CO** is expected to be relevant for a better understanding of the [FeFe]-hydrogenases chemistry; as an example, a direct comparison among the EPR spectra of the CO-inhibited enzymes with the spectra of biomimetic models showing the two alternative dispositions of CO and CN^- ligands around Fe_d could give crucial information not only on the influence exerted by ligands disposition on the EPR signals of biomimetic

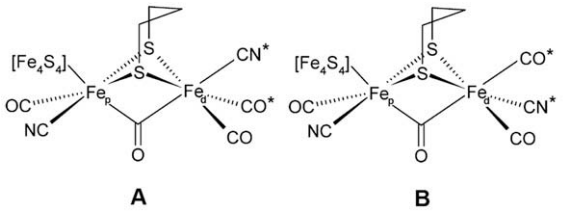

Scheme 2. CO-inhibited H-cluster structures as proposed by Zilberman et al. (model **A**), and its alternative geometry (Model **B**); the CO and CN^- groups that exchange their positions going from **A** to **B** are lebelled with an asterisk.

clusters, but also on the structure of CO-inhibited [FeFe]-hydrogenases. Indeed, different authors have recently described synthetic models of the CO-inhibited H-cluster [13,14]. The biomimetic complex that more closely reproduces the structure of the enzyme cofactor is $[Fe_2\{MeSCH_2C(Me)(CH_2S)_2\}(CN)_2(CO)_4]^{1-}$, an organometallic species recently obtained by Pickett and coworkers [13], which includes a bridging CO, as well as two terminal carbonyls and one CN^- group bound to Fe_d (see Scheme 3, in which the two most relevant isomers – **1** and **1′** – are represented; Fe_p corresponds to the iron center coordinated to the thioether ligand; the other iron atom is referred to as Fe_d, in analogy with the H-cluster). Because of such a close similarity between the enzyme diiron subcluster and $[Fe_2\{MeSCH_2C(Me)(CH_2S)_2\}(CN)_2(CO)_4]^{1-}$, this synthetic complex has been taken as the starting point for our investigation, the aim of which was twofold: (i) characterize the thermodynamically more stable $[Fe_2\{MeSCH_2C(Me)(CH_2S)_2\}(CN)_2(CO)_4]^{1-}$ isomer, by comparison of relative energies, as well as computed and experimental IR and EPR parameters of the synthetic cluster; (ii) probe the effect of prototypical ligands on the coordination environment of Fe_d in biomimetic models, an issue relevant for the design of tailored synthetic models of the **Hox-CO** form of the enzyme. To tackle the second point, a series of $[Fe_2(SCH_2\mathbf{X}CH_2S)(CN)_2(CO)_3(\mathbf{L})]^{n-}$ complexes, differing for the nature of **L**, which has been set to CO, $(CH_3)_2S$, CH_3S^-, CH_3O^- and F^-, and **X**, which has been set to CH_2, NH and O, has been investigated. It must be pointed out that the inclusion of very hard **L** ligands – like F^- and CH_3O^- – in the coordination environment of dinuclear models of the [FeFe]-hydrogenase active site is trivial in the context of DFT modelling, but obviously the same does not hold true for the synthetic chemist. Indeed, such complexes might not even correspond to stable species in solution. However, this has not to be considered a shortcoming, but instead a bonus associated to the computational investigation of models of the enzyme active site, since the goal of our study was not the computational design of novel synthetic complexes, but instead the disclosure of *general principles* that could be useful not only to drive the future design of novel synthetic models of **Hox-CO,** but also for planning and rationalizing experiments devoted to the characterization of possible structural rearrangements of the H-cluster in the **Hox-CO** form of the enzyme.

2. Computational details

DFT calculations have been carried out with the BP86 functional [15], using the resolution of identity technique [16] and an all-electron valence triple-ζ basis set with polarization functions on all atoms (TZVP [17]). Both geometry optimizations and atomic charge calculations have been carried out using the TURBOMOLE suite of programs [18]. The settings used for molecular electrostatic potential fitting are reported as Supplementary Information. B3LYP optimizations [19] – using the TZVP basis set – have been also carried out when IR frequency calculations had to be com-

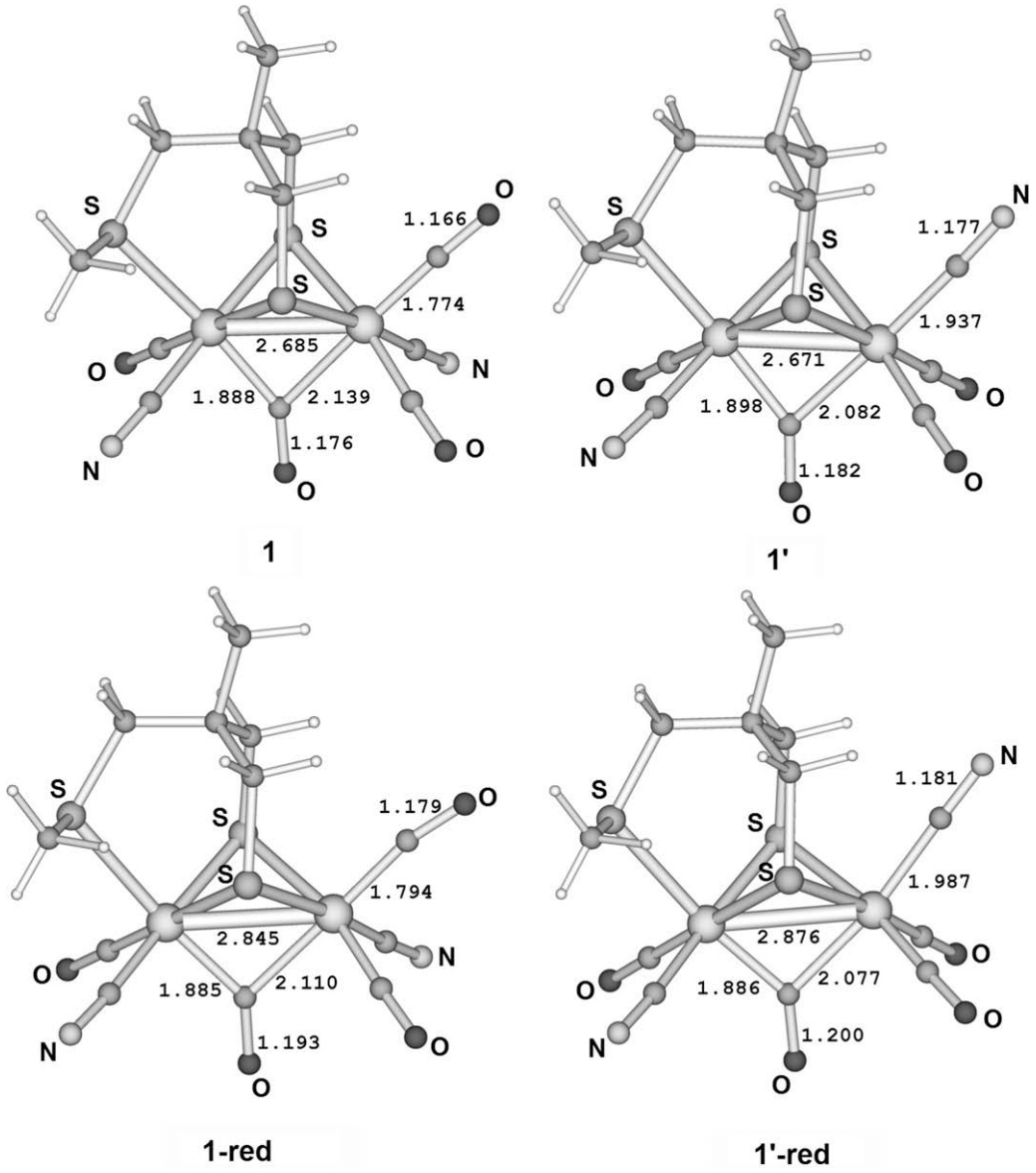

Fig. 1. BP86/TZVP optimized structures for **1**, **1′**, **1-red**, and **1′-red**. For the sake of clarity, only nitrogen, sulfur, and oxygen atoms are labelled, while hydrogen atoms (small size white spheres), carbon atoms (medium size grey spheres) and iron centers (large size, light grey spheres) are left unlabelled. Selected distances are given in Å.

puted, i.e. in the case of models **1, 1′**, and the corresponding mono-electron reduced isomers (**1-red** and **1′-red**, see Fig. 1).

Free energy (G) values have been obtained from the electronic SCF energy considering three contributions to the total partition function (Q), namely $q_{translational}$, $q_{rotational}$, and $q_{vibrational}$, under the assumption that Q may be written as the product of such terms [20]. In order to evaluate enthalpy and entropy contributions, the values of temperature and pressure have been set to 298.15 K and 1 bar, respectively. For the calculations of G values, the scaling factor for the SCF wavenumbers was set to 0.9 (the default value in the TURBOMOLE script FREEH, by means of which thermodynamics corrections are computed). Setting this parameter to 0.9914 (a value commonly applied with the BP86 functional) [21] or 0.9734 (which is widely used in the case of B3LYP calculations) [21] led to non-significant changes of no more than 0.05 kcal mol^{-1} in the computed ΔG values. Molecular rotations have been treated classically, and vibrational modes have been described according to the harmonic approximation.

Finally, computation of EPR parameters has been carried out using the MAG program [22].

3. Result and discussion

3.1. DFT investigation of the synthetic complexes $[Fe_2\{MeSCH_2C(Me)(CH_2S)_2\}(CN)_2(CO)_4]^{1-/2-}$

The experimental characterization of $[Fe_2\{MeSCH_2C(Me)(CH_2S)_2\}(CN)_2(CO)_4]^{1-}$ showed that this complex features carbonyl and cyanide IR-stretching frequencies which are very similar to those of the CO-inhibited [FeFe]-hydrogenases. Moreover, its EPR parameters fit well with the magnetic properties of CO-inhibited CpII [13]. However, due to its intrinsic instability, no X-ray data are at present available for such oxidized iron–sulfur synthetic assembly. In fact, two $[Fe_2\{MeSCH_2C(Me)(CH_2S)_2\}(CN)_2(CO)_4]^{1-}$ relevant isomers may exist; the first in which the CN^- ligand coordinated to Fe_d is in trans to the μ-CO group (**1**), and the second in which a CO ligand on Fe_d is in trans to the μ-CO group (**1′**) [23]. The unavailability of experimental structural data prevented shedding light on this ambiguity, and also prevented a direct comparison with the enzyme active site, until Zilberman et al. published a DFT study of the synthetic complex $[Fe_2\{MeSCH_2C(Me)$

$(CH_2S)_2\}(CN)_2(CO)_4]^{1-}$, based on the use of the PBE pure functional and plane-waves [24]. On the basis of a comparison between calculated and experimental IR data, Zilberman et al. concluded that the disposition of ligands in the model complex is such that the Fe_d-bound cyanide is *trans* to the CO group bridging the iron centers (adduct **1′** in Scheme 3). However, it is relevant to underline that, as recently noted by Hall and co-workers [8], the theoretical prediction of IR-stretching frequencies for μ-CO containing models can be a difficult task. Moreover, it was recently shown that structural assignment of the **Hox-CO** enzyme form based on comparisons between DFT and experimental IR-stretching frequencies have to be taken with caution, since the results are highly dependent on the functional used for the calculations [10].

Prompted by these observations, and with the aim of corroborating the previous structural assignments made by Zilberman et al., we initially carried out geometry optimization, IR-stretching frequencies and EPR parameters calculations for **1** and **1′** using both hybrid (B3LYP) and pure (BP86) functionals (see Methods; the BP86 optimized structures are shown in Fig. 1). To compare experimental and computational IR data, a linear regression fitting, in which only the terminally-bound diatomic ligands included in the cluster are considered, has been carried out. This choice was motivated by the observation that it is likely that the same scaling factor applies for the stretching modes of terminal CO ligands, while the stretching mode of the μ-CO group is expected to be much more sensitive to environmental effects, since the energy landscape associated with the movements of the μ-CO is very flat [25].

The calculated IR frequencies for **1** and **1′** are compared to the corresponding experimental data in Table 1. At BP86 level, it is not possible to reliably assess which DFT model better reproduces the experimental results, because the values of correlation coefficients (R^2) for isomers **1** and **1′** are too close to each other (R^2 = 0.948 and 0.936 for **1** and **1′**, respectively). Analogous considerations can be drawn for B3LYP vibrational frequencies; in this case, the correlation coefficients are even closer than those calculated with the BP86 functional (R^2 = 0.935 and 0.926 for **1** and **1′**, respectively). Therefore, our results confirm that structural assignment of models of the **Hox-CO** state based on comparisons between DFT and experimental IR-stretching frequencies can represent a difficult task for the computational chemist [8]. It should be noted that the difficulties do not arise from the open-shell nature of the synthetic complex, even though it is usually the case that the calculated IR spectra for open-shell compounds give poorer agreement with the experiment. In fact, the Fe(I)Fe(I) analogues of **1** and **1′** (complexes **1-red** and **1′-red**, see Fig. 1) are still very similar in terms of correlation coefficients, as far as their computed IR bands are compared with the corresponding experimental values from the dianion $[Fe_2(\mu\text{-CO})\{MeSCH_2C(Me)(CH_2S)_2\}(CN)_2(CO)_3]^{2-}$ (see Table 2).

The calculation of the free energy difference between the two isomers of the Fe(I)Fe(II) species indicates that the geometry corresponding to model **1′** is significantly favoured in a vacuum. In fact, the Fe(I)Fe(II) isomer with the CN^- ligand *trans* to the μ-CO is 5.75 kcal mol^{-1} and 5.05 kcal mol^{-1} lower in energy then the alternative conformation at BP86 and B3LYP levels, respectively. This result is in nice agreement with previous data obtained by Zilberman et al., who reported a 5.4 kcal mol^{-1} energy gap between **1** and **1′** [24]. However, it is relevant to note that the synthetic complex $[Fe_2\{MeSCH_2C(Me)(CH_2S)_2\}(CN)_2(CO)_4]^{1-}$ was experimentally synthesized and characterized in acetonitrile solution [13]; thus, we carried out the computation of free energy differences also by including solvation effects. It turned out that when the dielectric constant is set to the acetonitrile ε value (ε = 36.64; using the COSMO continuum solvent model, see Ref. [26]), the free energy difference between **1** and **1′** almost vanishes ($\Delta G_{\mathbf{1}-\mathbf{1}'}$ = 0.63 and 0.47 kcal mol^{-1} at BP86 and B3LYP level, respectively), not allowing the reliable prediction of the disposition of ligands around Fe_d. Finally, we also carried out the calculation of EPR parameters for **1** and **1′**, and compared the computed values with the corresponding experimental data [13]; the calculated **g** values for **1** and **1′** are reported in Table 3. The calculated EPR signals turned out to be rhombic for both **1** and **1′**, independently of the density functional used. However, EPR parameters computed on the basis of the BP86 wavefunctions turned out to be slightly closer to the experimental values then those obtained with B3LYP. More importantly, computed EPR values for **1** and **1′** are very similar to each other, again preventing to unravel the geometrical features of the synthetic cluster. Thus, it can be concluded that a definitive structural assignment of the mixed-valence diiron complex $[Fe_2(\mu\text{-CO})\{MeSCH_2C(Me)(CH_2S)_2\}(CN)_2(CO)_3]^{1-}$ using DFT calculations is not possible, and would require further experimental characterizations.

3.2. Effects of the modification of Fe_p coordination environment on Fe_d ligands disposition

As noted in Section 1, the design of tailored synthetic models of the **Hox-CO** form of the enzyme, i.e. featuring either a CO or a CN^- ligand on Fe_d *trans* to the bridging CO group, might be very useful

Table 1
Comparison between experimental and computed vibrational frequencies for isomers of the complex $[Fe_2\{MeSCH_2C(Me)(CH_2S)_2\}(CN)_2(CO)_4]^{1-}$.

Species	Terminal CO frequencies (cm^{-1})	CN^- frequencies (cm^{-1})	Linear regression	R^2
Experimental values[13]	1945, 1978, 2030	2083, 2107	–	–
1 (BP86)	1938, 1974, 1999	2115, 2131	$\nu_{exp} = 0.768\ \nu_{comp} + 468.4$	0.948
1′ (BP86)	1965, 1969, 2013	2110, 2113	$\nu_{exp} = 0.903\ \nu_{comp} + 192.7$	0.936
1 (B3LYP)	2045, 2069, 2097	2217, 2229	$\nu_{exp} = 0.770\ \nu_{comp} + 387.0$	0.935
1′ (B3LYP)	2060, 2067, 2105	2213, 2216	$\nu_{exp} = 0.853\ \nu_{comp} + 209.9$	0.926

Table 2
Comparison between experimental and computed vibrational frequencies for isomers of the complex $[Fe_2\{MeSCH_2C(Me)(CH_2S)_2\}(CN)_2(CO)_4]^{2-}$.

Species	Terminal CO frequencies (cm^{-1})	CN^- frequencies (cm^{-1})	Linear regression	R^2
Experimental values[13]	1878, 1919, 1957	2075, 2083	–	–
1-red (BP86)	1854, 1898, 1934	2068, 2101	$\nu_{exp} = 0.853\ \nu_{comp} + 300.7$	0.992
1′-red (BP86)	1891, 1899, 1951	2067, 2075	$\nu_{exp} = 1.029\ \nu_{comp} - 51.13$	0.984
1-red (B3LYP)	1949, 1976, 2019,	2175, 2197	$\nu_{exp} = 0.800\ \nu_{comp} + 332.4$	0.990
1′-red (B3LYP)	1968, 1984, 2033	2174, 2176	$\nu_{exp} = 0.907\ \nu_{comp} + 108.2$	0.988

Table 3
g-values of the complex $[Fe_2\{MeSCH_2C(Me)(CH_2S)_2\}(CN)_2(CO)_4]^{1-}$ with either apical CO (**1**) or apical CN (**1′**), computed either at B3LYP, or at BP86 level. Experimental results are shown in the last row.

	g_{11}	g_{22}	g_{33}	g_{iso}
B3LYP				
1	2.006	2.022	2.035	2.021
1′	2.011	2.015	2.037	2.021
BP86				
1	2.000	2.012	2.018	2.011
1′	1.999	2.011	2.017	2.008
Expt.	1.988	2.006	2.017	

in order to better understand the chemical properties of CO-inhibited [FeFe]-hydrogenases. To this end it is extremely important to understand if there are some stereoelectronic characteristics of the complex that could lead to the preferential formation of one of the isomers differing for the orientations of CO and CN^- ligands around the Fe_d center. In this context, theoretical investigations can be very useful, because they allow to efficiently sampling a wide variety of ligands without the inherent difficulties associated to synthetic efforts. In fact, such an issue can be tackled by means of a systematic study of theoretical model complexes differing in terms of the stereoelectronic properties of ligands coordinated to the iron centers. In addition, the investigation of a series of prototypical models of the **Hox-CO** form of the enzyme can complement previous studies aimed at disclosing stereochemical factors affecting the coordination geometry of diiron organometallic complexes resembling the [FeFe]-hydrogenase active site [27,28].

Prompted by the above observations, we have carried out DFT calculations (at BP86/TZVP level) on a series of models of general formula $[(CO)_2(CN)Fe_d(pdt)(\mu CO)Fe_p(CO)(CN)(\mathbf{L})]$, where **L** = CO, $(CH_3)_2S$, CH_3S^-, CH_3O^- and F^-. In other words, the ligand on Fe_p *trans* to the μ-CO has been systematically replaced by groups of increasing hardness, starting from the very soft CO group, up to the very hard F^- ligand. The optimized structures of the models investigated, as well as relevant geometrical parameters, are reported in Fig. 2 (**L** = CO in species **2** and **2′**, $(CH_3)_2S$ in species **3** and **3′**, CH_3S^- in species **4** and **4′**, CH_3O^- in species **5** and **5′** and F^- in **6** and **6′**). Notably, it turned out that the energy difference between the two isomers decreases moving from soft to hard Fe_p ligands: $\Delta G_{\mathbf{2'-2}} = -3.23$ kcal mol^{-1}, $\Delta G_{\mathbf{3'-3}} = -3.14$ kcal mol^{-1}, $\Delta G_{\mathbf{4'-4}} = -2.09$ kcal mol^{-1}, $\Delta G_{\mathbf{5'-5}} = -0.74$ kcal mol^{-1}, and $\Delta G_{\mathbf{6'-6}} = -0.73$ kcal mol^{-1}. In particular, if **L** is a hard ligand the energy difference between the two isomers becomes so small that it is not possible to reliably predict which disposition of ligands around Fe_d is preferred.

The analysis of the structural features of the investigated complexes can help rationalizing the observed trend. The Fe_p-C(μ-CO) distance decreases moving from **L** = CO to F^- (see Fig. 1), suggesting increased back-donation from Fe_p to CO moving along the series. In fact, in **2** and **2′** the Fe_p-C(μ-CO) distance is extremely long due to the competition of the two trans CO ligands coordinated to Fe_p. Replacing **L** = CO with better sigma-donor ligands such as $(CH_3)_2S$ and CH_3S^- makes Fe_p more electron rich and consequently more suited to back-donate to the semibridging CO. Notably, the Fe_p-C(O) distance becomes even shorter when **L** = CH_3O^- and F^-, which, due to the electronegativity of the O and F atoms can hardly be considered better sigma-donors than S ligands. When **L** = CH_3O^- and F^- a more realistic representation of the observed behaviour can be drawn considering that F and O atoms polarize the Fe_p atoms, pushing electrons away from the Fe_p–L bond and consequently favouring back-donation to the bridging CO. The polarization effect induced by very hard ligands could be invoked to explain the movement of the μ-CO towards Fe_p also on the basis of purely electrostatic considerations; actually, the carbon atom of the μ-CO ligand is electrophilic in all the Fe(I)Fe(II) complexes (see Supporting Information). Thus, the shortening of the bond distance between the C atom of the bridging carbonyl and a strongly polarized proximal metal center is expected to be favoured. In any case, the movement of μ-CO toward Fe_p selectively stabilize **n** vs. **n′** isomers, because the competition between trans CO ligands coordinated to Fe_d is relieved when μ-CO moves toward Fe_p. This scenario is corroborated by the observation that the distances between Fe_d and the terminal CO in *trans* to μ-CO decrease (suggesting stronger back-donation) moving from **L** = CO to **L** = F^-.

3.3. Effects of the modification of the pendant on Fe_d-bound ligands disposition: the inclusion of di(thiomethyl)ether (dtme) or di(thiomethyl)amine (dtma) in place of pdt

The development of strategies devoted to the tailoring of the Fe_d coordination environment in **Hox-CO** synthetic models could also take advantage from the different electronic properties of CO and CN^- ligands. In fact, the Fe_d-bound CN^- ligand is expected to maintain a significant anionic character even when coordinated to the metal center, while CO ligands should be close to neutrality. These qualitative considerations are supported by the computed partial charges for complexes **1–6** and **1′–6′** (Supporting Information). This observation suggests that modifications in the Fe_d second coordination sphere could be helpful for modulating CO and CN^- ligands arrangement around Fe_d. In particular, the presence of a chelating ligand including an electronegative atom in place of the β carbon atom of pdt could, in principle, destabilize isomers in which the Fe_d coordination site *trans* to the μ-CO group is occupied by a negatively charged cyanide group. In this context, it is noteworthy that Szilagyi and coworkers [29] have recently proposed that the chelating group in [FeFe]-hydrogenase could be di(thiomethyl)ether (dtme), which includes an oxygen atom in place of the β carbon of pdt. In fact, the replacement of pdt with dtme in our model complexes did not lead to a significant stabilization of isomers carrying a carbonyl *trans* to the μ-CO on Fe_d, probably because the ether oxygen is not sufficiently close to the ligand trans to the μ-CO on Fe_d, to establish intramolecular interactions which are significantly different in the two cases.

Since several mechanicistics considerations and spectroscopic results point towards the presence of dtma as the chelating ligand [11], we also carried the DFT study of model complexes analogous to **2–6**, but differing for the presence of a di(thiomethyl)amine (dtma) in place of pdt (complexes **2-DTMA – 6-DTMA** and **2′-DTMA – 6′-DTMA**, see Fig. 3). The presence of an amine group in the pendant ligand might lead to the formation of an intramolecular hydrogen bond between the NH group of the pendant an the Fe_d-bound CN^- group, when the latter is *trans* to the μ-CO; thus, a preferential stabilization of such disposition of ligands might result in dtma-containing complexes. In fact, all the complexes featuring a CN^- group *trans* to the μ-CO (adducts **2′-DTMA – 6′-DTMA**) were computed to be significantly lower in energy then the corresponding isomers featuring two carbonyls *trans* to each other on Fe_d (adducts **2-DTMA – 6-DTMA**). Notably, the free energy differences – $\Delta G_{\mathbf{2'\text{-}DTMA\text{–}2\text{-}DTMA}} = -6.53$ kcal mol^{-1}, $\Delta G_{\mathbf{3'\text{-}DTMA\text{–}3\text{-}DTMA}} = -6.74$ kcal mol^{-1}, $\Delta G_{\mathbf{4'\text{-}DTMA\text{–}4\text{-}DTMA}} = -3.74$ kcal mol^{-1}, $\Delta G_{\mathbf{5'\text{-}DTMA\text{–}5\text{-}DTMA}} = -2.64$ kcal mol^{-1}, and $\Delta G_{\mathbf{6'\text{-}DTMA\text{–}6\text{-}DTMA}} = -2.20$ kcal mol^{-1} – are always larger then the corresponding energy gaps for pdt-containing models.

As for the effects of the presence of harder ligand on Fe_p *trans* to the μ-CO, it is confirmed that they tend to maintain the μ-CO closer to Fe_p. In the case of complexes **5-DTMA** and **6-DTMA**, this effect is particularly pronounced: in fact, the μ-CO ligand moves so far from Fe_d (~3 Å), in both **5-DTMA** and **6-DTMA**, and the Fe_p–C–O angle is so close to 180° (167.6° and 170.2°, respectively), that it can be

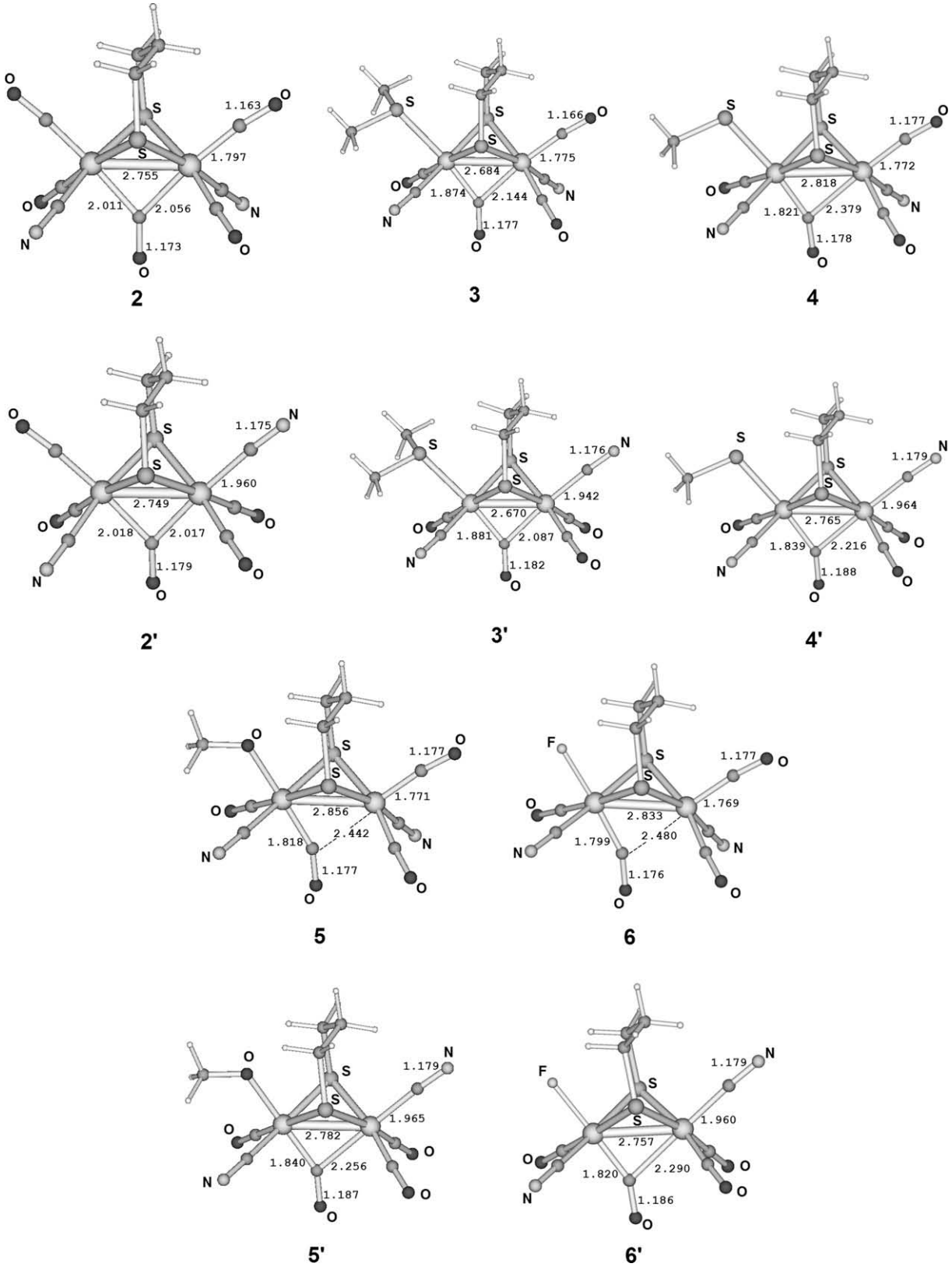

Fig. 2. DFT optimized structures for **2**, **2′**, **3**, **3′**, **4**, **4′**, **5**, **5′**, **6** and **6′**. For the sake of clarity, only nitrogen, sulfur, oxygen and fluorine atoms are labelled, while hydrogen atoms (small size white spheres), carbon atoms (medium size grey spheres) and iron centers (large size, light grey spheres) are left unlabelled. Selected distances are given in Å.

considered to be terminally coordinated to Fe_p. Finally, it is found that the inclusion of softer Fe_p ligands favours isomers in which a CN^- ligand is in *trans* to the μ-CO on Fe_d, similarly to what observed with pdt-containing complexes.

4. Conclusions

In this work some properties of complexes structurally related to the CO-inhibited form of the H-cluster have been characterized

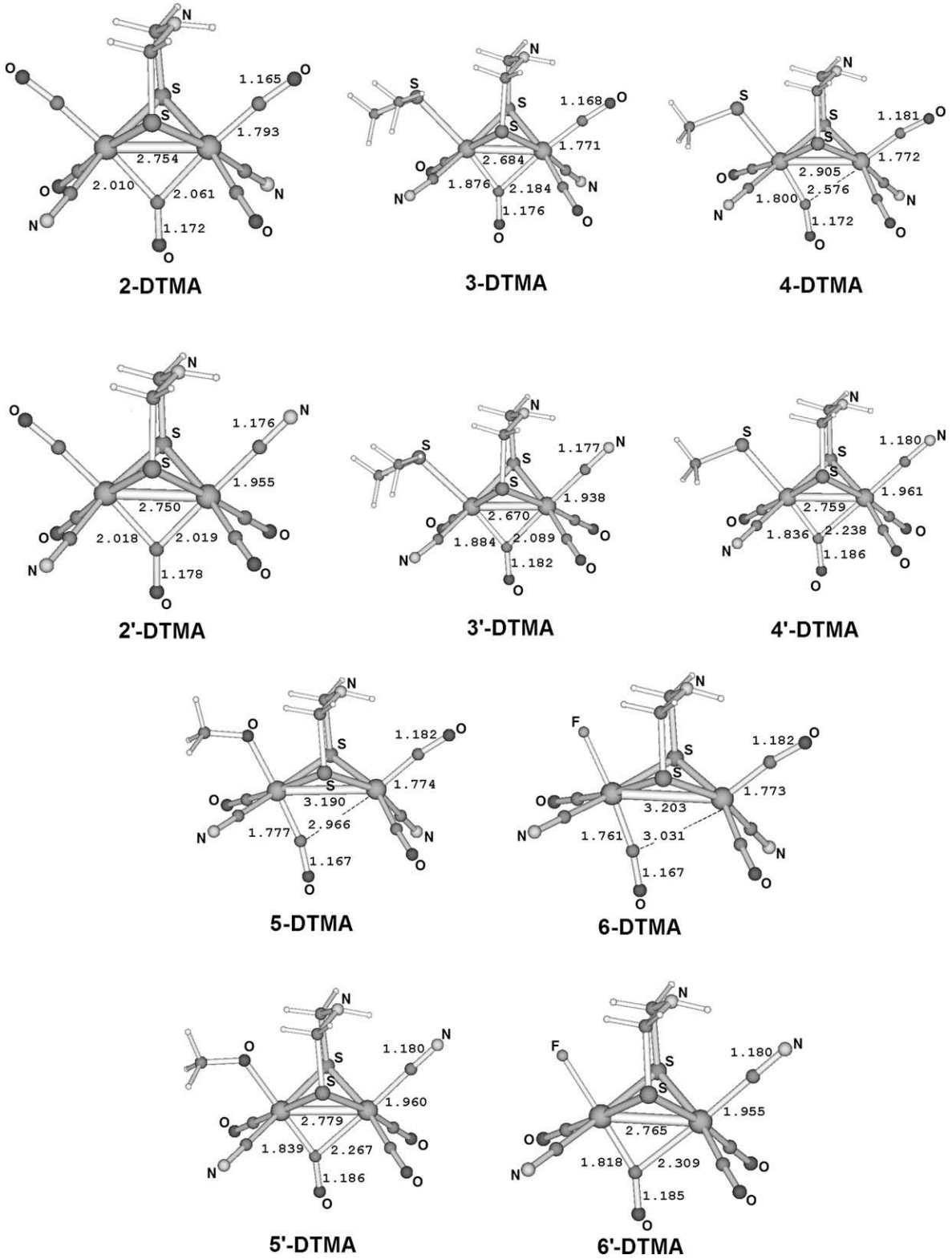

Fig. 3. DFT optimized structures for **2-DTMA**, **2′-DTMA**, **3-DTMA**, **3′-DTMA**, **4-DTMA**, **4′-DTMA**, **5-DTMA**, **5′-DTMA**, **6-DTMA** and **6′-DTMA**. For the sake of clarity, only nitrogen, sulfur, and oxygen atoms are labelled, while hydrogen atoms (small size white spheres), carbon atoms (medium size grey spheres) and iron centers (large size, light grey spheres) are left unlabelled. Selected distances are given in Å.

using DFT calculations. As a first step, we computed the IR and EPR parameters of $[Fe_2\{MeSCH_2C(Me)(CH_2S)_2\}(CN)_2(CO)_4]^{1-}$, a synthetic compound that, in analogy with [FeFe]-hydrogenase active site, features a CO group bridging the metal centers and a thioether sulfur ligand bound to the proximal iron atom. The comparison between computed and experimental IR and EPR data, together with the calculation of free energy differences between the relevant isomers, showed that a complete characterization of the structural

properties of this synthetic compound is a non-trivial task. This observation prompted us to study the general principles underlying the stabilization of the alternative orientations of CO and CN^- ligands around the Fe_d center in models of the enzyme cofactor, investigating a series of related pdt-containing model compounds. The computed trend in relative stabilities clearly indicates that the inclusion of hard ligands in the Fe_p coordination sphere could be a viable strategy to selectively favour isomers featuring two CO groups *trans* to each other on Fe_d. The substitution of pdt with a dtma residue leads to the selective stabilization of the configuration of Fe_d-bound ligands in which a CN^- ligand is *trans* to μ-CO, thanks to the formation of an intramolecular hydrogen bond between the amine group of the pendant and the Fe_d-bound CN^- ligand. Notably, the presence of hard ligands on Fe_p affected the Fe_d coordination environment also in the case of dtma-containing complexes: in fact, the energy difference between the dtma-containing isomers showing either a CN^- or a CO group trans to the μ-CO decreased from ~6.5 to ~2 kcal mol^{-1}, when **L** = CO and F^-, respectively.

As a final remark, it is worth pointing out that to date there are limited cases where the exact stereochemistry of dithiolate-bridged dicyanide carbonyl compounds is known with confidence. The results of our work might give useful suggestions to design synthetic diiron complexes characterized by tailored stereochemical arrangements of ligands around the metal centers. More generally, theoretical studies and the recent advances in the design of chelating and/or bulky ligands which are able to specifically bind one of the metal centers in bioinspired Fe(I)Fe(II) model complexes [14] will hopefully open new perspectives for the synthesis of tailored synthetic models of the **Hox-CO** form of the enzyme.

Acknowledgement

C.G. acknowledges support from the Alexander von Humboldt foundation.

Appendix A. Supplementary material

Supplementary data associated with this article can be found, in the online version, at doi:10.1016/j.jorganchem.2009.03.007.

References

[1] M.Y. Darensboug, Nature 433 (2005) 589–591.
[2] J.W. Peters, W.N. Lanzilotta, B.J. Lemon, L.C. Seefeldt, Science 282 (1998) 1853–1858.
[3] Y. Nicolet, C. Piras, P. Legrand, C.E. Hatchikian, J.C. Fontecilla-Camps, Structure 7 (1999) 13–23.
[4] (a) F.A. Armstrong, Curr. Opin. Chem. Biol. 8 (2004) 133–140;
(b) Y. Nicolet, B.J. Lemon, J.C. Fontecilla-Camps, J.W. Peters, Trends Biochem. Sci. 25 (2000) 138–143.
[5] I.C. Zambrano, A.T. Kowal, L.E. Mortenson, M.W.W. Adams, M.K. Johnson, J. Biol. Chem. 264 (1989) 20974–20983;
G. Wang, M.J. Benecky, B.H. Huynh, J.F. Cline, M.W.W. Adams, L.E. Mortenson, B.M. Hoffman, E. Munck, J. Biol. Chem. 259 (1984) 14328–14331;
J. Tesler, M.J. Benecky, M.W.W. Adams, L.E. Mortenson, B.M. Hoffman, J. Biol. Chem. 261 (1986) 13536–13541;
B.J. Lemon, J.W. Peters, Biochemistry 38 (1999) 12969–12973;
A.S. Pereira, P. Tavares, I. Moura, J.J.G. Moura, B.H. Huynh, J. Am. Chem. Soc. 123 (2001) 2771–2782.
[6] A.L. De Lacey, C. Stadler, C. Cavazza, E.C. Hatchikian, V.M. Fernandez, J. Am. Chem. Soc. 122 (2000) 11232–11233.
[7] I.P. Georgakaki, L.M. Thomson, E.J. Lyon, M.B. Hall, M.Y. Darensbourg, Coord. Chem. Rev. 238 (2003) 255;
A.T. Fiedler, T.C. Brunold, Inorg. Chem. 44 (2005) 9322–9334;
Z. Cao, M.B. Hall, J. Am. Chem. Soc. 123 (2001) 3734–3742.
[8] J.W. Tye, M.Y. Darensbourg, M.B. Hall, J. Comput. Chem. 27 (2006) 1454–1462.
[9] S. Zilberman, E.I. Stiefel, M.H. Cohen, R. Car, Inorg. Chem. 45 (2006) 5715–5717.
[10] C. Greco, M. Bruschi, J. Heimdal, P. Fantucci, L. De Gioia, U. Ryde, Inorg. Chem. 46 (2007) 7256–7258.
[11] W. Lubitz, Book of Abstracts of the 2007 International Hydrogenase and Hydrogen Production Conference, p. 17 and 143;
Y. Nicolet, A.L. De Lacey, X. Vernede, V.M. Fernandez, E.C. Hatchikian, J.C. Fontecilla-Camps, J. Am. Chem. Soc. 123 (2001) 1596–1601;
H.J. Fan, M.B. Hall, J. Am. Chem. Soc. 123 (2001) 3828–3829.
[12] B. Bennett, B.J. Lemon, J.W. Peters, Biochemistry 39 (2000) 7455–7460;
D.S. Patil, B.H. Huynh, S.H. He, H.D. Peck, D.V. Dervartanian, J. Legall, J. Am. Chem. Soc. 110 (1988) 853–8534;
M.W.W. Adams, J. Biol. Chem. 262 (1987) 15054–15061;
J. Telser, M.J. Benecky, M.W.W. Adams, L.E. Mortenson, B.M. Hoffman, J. Biol. Chem. 262 (1987) 6589–6594;
A. Silakov, E.J. Reijerse, S.P.J. Albracht, E.C. Hatchikian, W. Lubitz, J. Am. Chem. Soc. 129 (2007) 11447–11458;
S.P.J. Albracht, W. Roseboom, C. Hatchikina, J. Biol. Inorg. Chem. 11 (2006) 88–101.
[13] M. Razavet, S.J. Borg, S.J. George, S.P. Best, S.A. Fairhurst, C.J. Pickett, Chem. Commun. (2002) 700–701.
[14] A.K. Justice, T.B. Rauchfuss, S.R. Wilson, Angew. Chem., Int. Ed. 46 (2007) 6152–6154;
A.K. Justice, L. De Gioia, M.J. Nilges, T.B.. Rauchfuss, S.R. Wilson, G. Zampella, J. Am. Chem. Soc. 47 (2008) 7405–7414;
A.K. Justice, M.J. Nilges, T.B. Rauchfuss, S.R. Wilson, L. De Gioia, G. Zampella, J. Am. Chem. Soc. 47 (2008) 529–5301.
[15] A.D. Becke, Phys. Rev. A 38 (1988) 3098–3100;
J.P. Perdew, Phys. Rev. B 33 (1986) 8822–8824.
[16] K. Eichkorn, O. Treutler, H. Öhm, M. Haser, R. Ahlrichs, Chem. Phys. Lett. 240 (1995) 283–289;
K. Eichkorn, F. Weigend, O. Treutler, R. Ahlrichs, Theor. Chem. Acc. 97 (1997) 119–124.
[17] A. Schafer, C. Huber, R. Ahlrichs, J. Chem. Phys. 100 (1994) 5829–5835.
[18] R. Ahlrichs, M. Bar, M. Haser, C. Horn, C. Kolmel, Chem. Phys. Lett. 162 (1989) 165–169.
[19] A.D. Becke, J. Chem. Phys. 98 (1993) 5648–5652;
P.J. Stephens, F.J. Devlin, C.F. Chabalowski, M.J. Frisch, J. Phys. Chem. 98 (1994) 11623–11627.
[20] F. Jensen, Introduction to Computational Chemistry, John Wiley and Sons Ltd., Chichester, UK.
[21] C.J. Cramer, Essentials of computational chemistry, Theories and Models, Wiley, New York, 2002.
[22] V.G. Malkin, O.L. Malkina, L. Reviakine, A.V. Arbouznikov, M. Kaupp, B. Schimmelpfennig, I. Malkin, T. Helgaker, K. Ruud, RESPECT Program, Version 1.1.
[23] In principle, another isomer of **1** is conceivable, in which the CN^- bound to Fe_d is in cis with respect to the Fe_p-bound CN^- ligand (taking the Fe–Fe axis as a reference). However, this alternative isomer is, at BP86/TZVP level, so similar to **1**, in terms of relative stability ($\Delta G < 1$ kcal mol^{-1}) and IR absorption features (the difference between terminal CO and CN^- computed normal modes never exceeded the value 6 cm^{-1}), that we decided not to take it explicitly into account in the present study.
[24] S. Zilberman, E.I. Stiefel, M.H. Cohen, R. Car, J. Phys. Chem. B 110 (2006) 7049–7057.
[25] C. Greco, M. Bruchi, L. De Gioia, U. Ryde, Inorg. Chem. 46 (2007) 5911–5921.
[26] A. Klamt, J. Phys. Chem. 99 (1995) 2224–2235;
A. Klamt, J. Phys. Chem. 100 (1996) 3349–3353.
[27] M. Bruschi, P. Fantucci, L. De Gioia, Inorg. Chem. 42 (2003) 4773–4781;
M. Bruschi, P. Fantucci, L. De Gioia, Inorg. Chem. 43 (2004) 3733–3741.
[28] M.Y. Darensbourg, E.J. Lyon, X. Zhao, I.P. Georgakaki, Proc. Natl. Acad. Sci. USA 100 (2003) 3683;
I.P. Georgakaki, L.M. Thomson, E.J. Lyon, M.B. Hall, M.Y. Darensbourg, Coord. Chem. Rev. 238–239 (2003) 255.
[29] A.S. Pandey, T.V. Harris, L.J. Giles, J.W. Peters, R.K. Szilagyi, J. Am. Chem. Soc. 130 (2008) 4533–4540.